Journal of Sustainable Mining 18 (2019) 270–276

HOSTED BY

ELSEVIER

Contents lists available at ScienceDirect

Journal of Sustainable Mining

journal homepage: www.elsevier.com/locate/jsm

Research article

Investigation on fire potential of ventilation ducts

Ankit Jha[a,*], Vinod Amar[b], Purushotham Tukkaraja[a]

[a] Department of Mining Engineering and Management, South Dakota School of Mines and Technology, United States
[b] Department of Chemical and Biological Engineering, South Dakota School of Mines and Technology, United States

ARTICLE INFO

Keywords:
Auxiliary ventilation
Heat release rate
Emission factor
Differential scanning calorimetry
Thermogravimetric analysis

ABSTRACT

Fires in underground mines can create dangerous conditions for personnel and cause severe damage to property. Because of the confined nature of the underground environment, these effects can escalate rapidly. In underground mines, air ducts/bags are used for ventilating narrow blind headings; these consist of combustible materials that have not been investigated thoroughly in terms of their fire potential and gas emissions. The primary objective of this study is to investigate the fire potential and emission factors for these ducts. A preliminary investigation was performed using differential scanning calorimetry and thermogravimetric analysis. These tests provide crucial information for duct samples including the melting point which is used for designing a novel experimental setup for combustion analysis. This setup was used to perform a combustion experiment at 350 °C, so that all specimens can achieve complete combustion. Furthermore, the heat release rate and emission factors were calculated; it was observed that heat release rate for all the specimens was identical because of similar oxygen consumption during the experiment. Sample B has the lowest emission factor among the four samples (A, B, C, D) tested in this study.

1. Introduction

Underground mining offers a lot of challenges in terms of the risks associated with fires, toxic contaminants, gas explosions, roof falls, and inundation (Dozolme, 2019). The effects of these hazards escalate rapidly due to the confined nature of underground mines. Although in recent years, significant improvement in mine health and safety has been achieved, accidents still occur. While 2008 is the second-lowest year of fatalities ever recorded (MSHA, 2019) with 27, it is still imperative to engage in further improvements and ongoing efforts to strive and achieve a better standard with even lower rates of fatalities and injuries.

This study focuses on fire hazards in underground mines. There are several combustible materials that can potentially support fires in the underground environment. The heat and noxious gases produced by the fire can be life threatening, as the atmosphere can become toxic rapidly if the fire is not controlled. Although these combustible materials are usually manufactured using fire-resistant materials, previous studies have shown that fires can still occur and propagate through underground openings; an experimental study shows that fire could spread through conveyor belt material at rates of more than 20 fpm (Lazzara & Perzak, 1990). A total of 137 fire accidents have been recorded in underground metal/nonmetal mines from 1991 to 2000 in the United States (Conti, Chasko, Wiehagen, & Lazzara, 2005). A study published by NIST states that electric short-circuiting/arching was a major cause of fire accidents occurred between 1990 and 1999 in the United States (De Rosa, 2004). A research study on the preparedness of underground miners at seven coal mines indicated that around 38% of miners had been ordered to evacuate once or more (Conti et al., 2005). Several researchers have performed investigations on mine fires in terms of understanding the fire characteristics, response preparedness, and modeling of the fire situation (Prosser et al., 2017; Conti, 2001; Conti et al., 2005; Rosa, 2004; Trevits, Yuan, Smith, & Thimons, 2008). The U.S. Bureau of Mines investigated products of combustion obtained from flammable materials used in coal mines; these materials include wood, the transformer fluid, coal, brattice cloth, and ventilation ducting. These were all tested in a ventilated fire tunnel. This study investigated the effect of various parameters on the combustion process, including ventilation rate, mass loss rate, gas concentration, light transmission, as well as smoke particulate mass, number, and concentration. Consequently, several recommendations were made in terms of the effect of smoke and gas produced from all the material considered for this study, in order to accomplish better emergency planning. Furthermore, the results obtained from this study were used in the development of a sensor to detect fire events (Egan, 1990). The Center for Disease Control (CDC) published an information circular that outlines necessary preparation and response measures to be taken during a fire event in a mine (Conti et al., 2005). Another study concerning the fire situation in roadways and tunnels was discussed and the

* Corresponding author.
E-mail address: ankitkrjha@gmail.com (A. Jha).

https://doi.org/10.1016/j.jsm.2019.11.002
Received 27 August 2019; Received in revised form 16 October 2019; Accepted 28 November 2019
Available online 02 December 2019

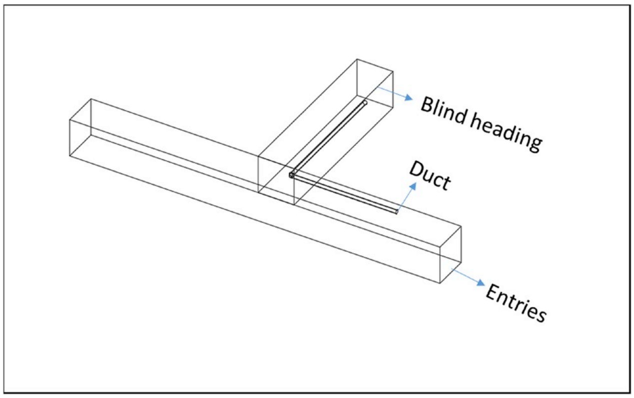

Fig. 1. Auxiliary ventilation in blind heading.

importance of incorporating design features for fire events in tunnel planning was emphasized. Also, the emergency ventilation systems to be used during a fire situation were discussed (Duckworth, 2008). Several commercial and research organizations have developed software packages for modeling fire under different scenarios (Consulting; Mining Product: MFIRE; NIST). All the underground mines are ventilated to provide fresh air to the miners and to dilute contaminant concentrations to safe permissible limits (McPherson, 2012). The ventilation in these mines is accomplished using fans situated at the surface, underground or both. One of the techniques to accomplish ventilation in blind headings is using an auxiliary ventilation system, which consists of a line brattice or a fan and duct system. Predominantly, the fan and duct system is preferred over line brattice due to better ventilation control and no additional increase in the mine resistance (McPherson, 2012). Fig. 1 shows the schematic of a blind heading; usually a fan is connected to the end of the duct towards the entries, which directs air into the blind heading. The most common material used for auxiliary ventilation ducting is coated steel, alloyed steel, fiberglass, and resin (McPherson, 2012). Fire modeling studies for underground mines are helpful in understanding the consequences of fire events under given conditions. Additionally, conducting sensitivity analysis for different fire conditions helps to ensure miners are prepared to respond to the emergency. To this purpose, a few studies have demonstrated the utility of fire simulation for underground mines using commercial ventilation software. Fire situations at three locations, including a fuel bay, magazine, and conveyor were simulated and their effect in terms of carbon-monoxide concentration, visibility, and airflow reversal was examined (Brake, 2013). A situation with multiple underground mine fires involving 17 fire risk scenarios was simulated for Freeport's Indonesia underground operations. The main objective of this study was to accomplish a fire risk assessment for transitioning an open-pit mine into an underground block caving operation. Additionally, video animation for these simulations was developed to communicate the fire risk to stakeholders. However, this exercise did not include a fire situation involving ventilation ducts. Furthermore, several research publication in mine ventilation engineering were completed to investigate fire, explosion, and related hazards in underground mines (Ajitha et al., 2019; Arya, Novak, Saito, Levy, & Sottile, 2019; Gangrade, Schatzel, & Harteis, 2019; Jha, Calizaya, & Nelson, 2015; Jha & Tukkaraja, 2019; Kumar, Wedding, Jolly, Arya, & Novak, 2016).

This paper aims to investigate the fire potential of four different ventilation ducts. Two objectives are accomplished in this study: 1) The calculation of heat generation from the combustion of ventilation ducts, and 2) Evaluation and calculation of emission factors for the products of combustion. These two parameters are used as inputs in commercial ventilation software in order for comprehensive fire modeling to be accomplished. To achieve these two broad objectives, thermogravimetric analysis, and differential scanning calorimetry was used to evaluate the physical and chemical properties of the materials. In addition a novel experimental setup was utilized when performing the combustion experiment to obtain the heat of combustion and the emission factor for ventilation ducts.

2. Preliminary investigation

Four ventilation ducts commonly used in underground mines for auxiliary ventilation were used for this study. Fig. 2 shows the pictures of these duct materials, hereinafter these are referred to as “specimens”.

2.1. Differential scanning calorimetry

Differential scanning calorimetry (DSC) is commonly used in identifying phase transition, including melting point, glass transition, and exothermic decomposition.

Heat capacity and energy changes are detected by DSC with great precision. At phase transition the heat capacity of specimen changes convert to heat flow information. In the DSC experiment, heat flows from the furnace to the specimen and is measured relative to the reference (Alagarsamy, 2016a). Although DSC does not identify the physical composition of these

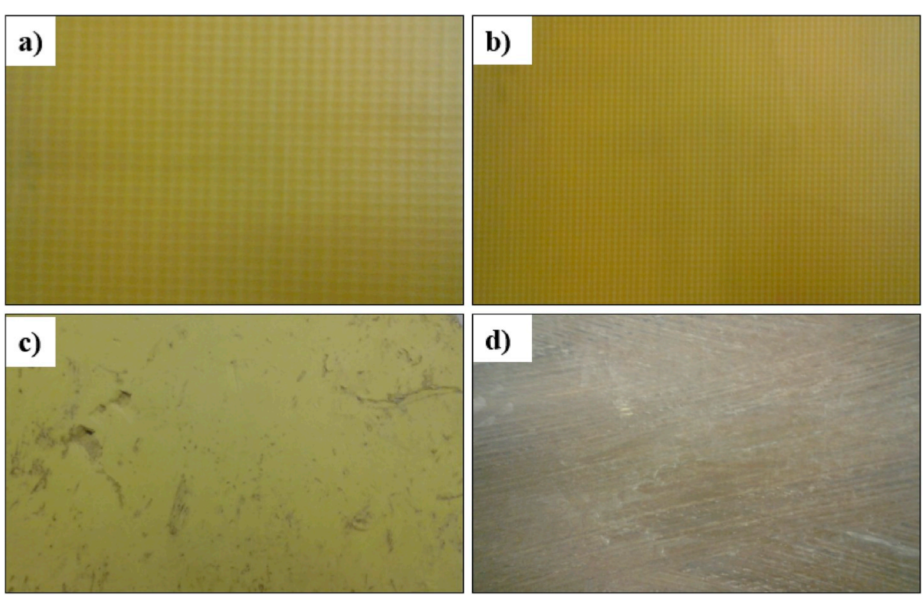

Fig. 2. a) Specimen A, (b) Specimen B, c) Specimen C and d) Specimen D.

ducts, crucial information, such as glass transition temperature, crystallization temperature, and melting point, can be acquired using the experiment (Wikipedia). In DSC, two pans are used for measurement, one is the reference pan and the other one is the specimen holder. The specimen and reference crucible are identical, except for the fact that the reference crucible is empty, whereas the specimen crucible contains the specimen. All the information related to heat flowing in and out of the specimen is recorded by sensors and can be plotted on a graph. The information obtained from the graph includes enthalpy of melting, melting point, and specific heat capacity (Laboratory, 2012). The first event in the graph is the glass transition of material and can be observed as a step in the curve, this is followed by the exothermic crystallization peak and the endothermic melting peak. The information of interest for this study was the melting point of the material. The beginning and end of the negative peak indicate the start and finish of the melting phase, both of these temperatures were recorded for further analysis. For the purposes of this study, the SDT Q 600 instrument was used which provides simultaneous measurement of weight change and true differential heat flow (Thermal Analysis Instruments, 2010). This procedure was conducted for all the specimens. Fig. 3a–d shows the DSC results for specimens A, B, C, and D respectively. The melting point for specimens A, B, and C was determined as 284 °C, 284 °C, and 273 °C, respectively. There was no noticeable peak for specimen D, indicating absence of the melting phase even at higher temperatures.

2.2. Thermogravimetric analysis

Thermogravimetric analysis involves the study of the mass change of a material as a function of temperature or time (Alagarsamy, 2016c). TGA analysis is indicative of the temperature of the decomposition of the material, which is defined as the temperature at which onset of mass change in the specimen is observed. Furthermore, the graphs obtained during the analysis can classify the materials in different ways according to their shapes. The sample environment is controlled by the sample purge gas. The purge gas can be inert or reactive depending on the goals of the experiment and flows over the sample to finally exit through an exhaust (PerkinEmler). Nitrogen was used as the purge gas for this study, with the temperature programmed to increase at 20 °C/min. Fig. 4a–d shows the TGA results for specimens A, B, C, and D, respectively.

For specimen A, B, and C multi-stage decomposition was detected, whereas, for sample D no mass change was observed indicating that decomposition temperature is greater than the temperature range of the instrument (Alagarsamy, 2016b).

3. Experimental setup and investigation

Initial investigation of the specimens using DSC and TGA provided crucial physical characteristics for establishing experimental parameters. An experimental setup was made consisting of a furnace, a glass tube, a crucible, compressed air cylinder, and a gas detector. The furnace is required to maintain the temperature needed to support combustion of the specimens. The furnace is capable of maintaining a temperature of 1500 °C. The specimens are placed on the crucible and positioned at the center of the glass tube within the furnace. One end of the glass tube is connected to the compressed air cylinder providing air to support combustion, while the other end is connected to the gas detector for measuring products of combustion. The glass tube is 4 ft in length and has an internal diameter of 1.8 inches. Both sides of the glass tube are sealed with a steel tube where an arrangement was made to supply air into the chamber through one end of the tube and make the gas concentration measurements at the other end.

The airflow through the compressed air cylinder was established at 6.66e–06 m^3/s with an objective of providing oxygen to support combustion. Based on the results obtained from DSC and TGA analysis the furnace temperature was maintained at 350 °C, which was well above the melting point of all the specimens. In this study, Mine Safety Appliance (MSA) Altair 5-X gas detector was utilized to monitor gas concentrations during the combustion process. This detector is capable of sensing six gases including oxygen, carbonmonoxide, carbon dioxide, hydrogen sulfide, nitrogen dioxide, and combustible. The detection range for the gases are 0–30% Vol with 0.1% resolution for oxygen, 0–2000 ppm with 1 ppm resolution for carbon-monoxide, 0–10,000 ppm with 5 ppm resolution for carbon-dioxide, 0–200 ppm with 1 ppm resolution for hydrogen sulfide, and 0–100% with 1% LEL for combustible (Alagarsamy, 2016b). Fig. 5 shows the experimental setup used for this study. Initially, 0.2 g of each specimen was used for the combustion experiment. The detector has data logging capabilities designed to monitor and store data with a minimum count of 15 s. The combustion product was sampled for the entire duration of the experiment until no detectable gases were observed. Upon completion of the combustion experiment, concentration within the glass tube reverts to the normal concentration of general air. At this point, the specimens are presumed to have achieved complete combustion. Specimens were weighed after completion of the experiment to obtain the mass of the dry fuel consumed.

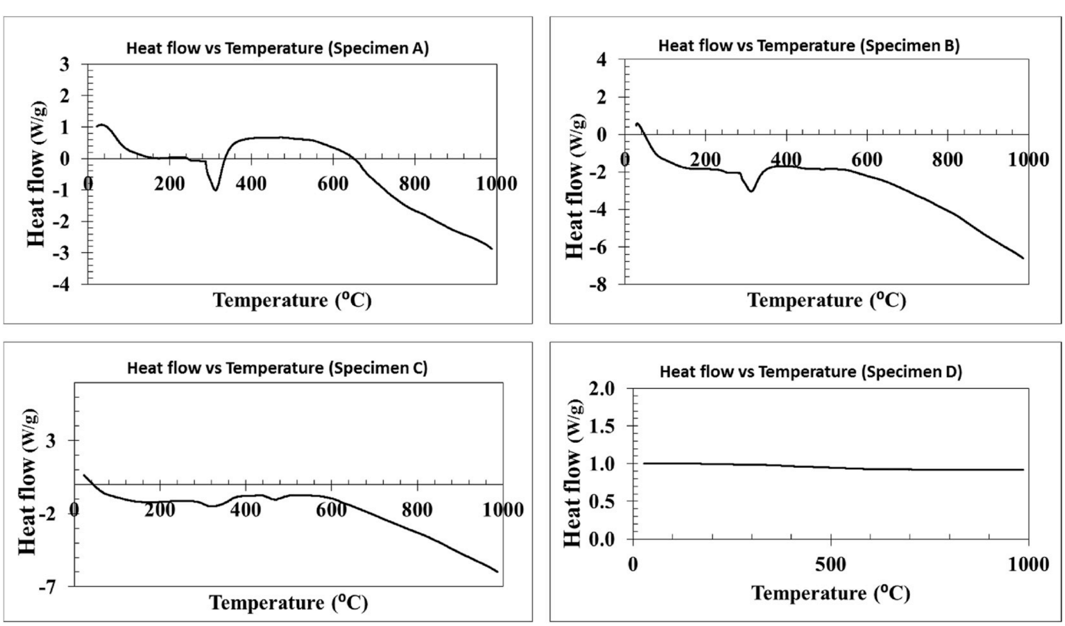

Fig. 3. DSC profiles for a) Specimen A, b) Specimen B, c) Specimen C and d) Specimen D, respectively.

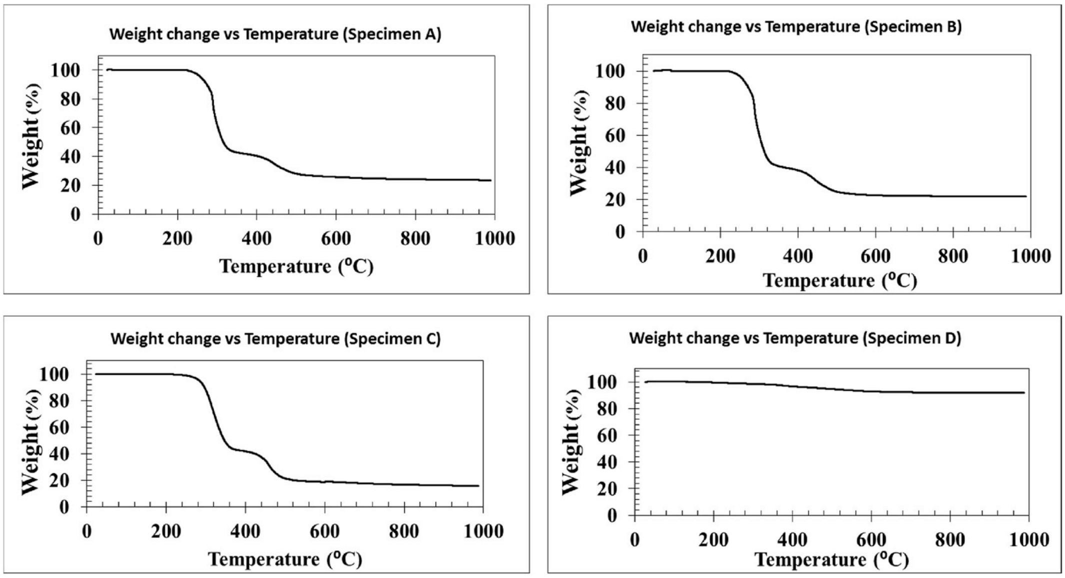

Fig. 4. TGA profiles for a) Specimen A, b) Specimen B, c) Specimen C and d) Specimen D.

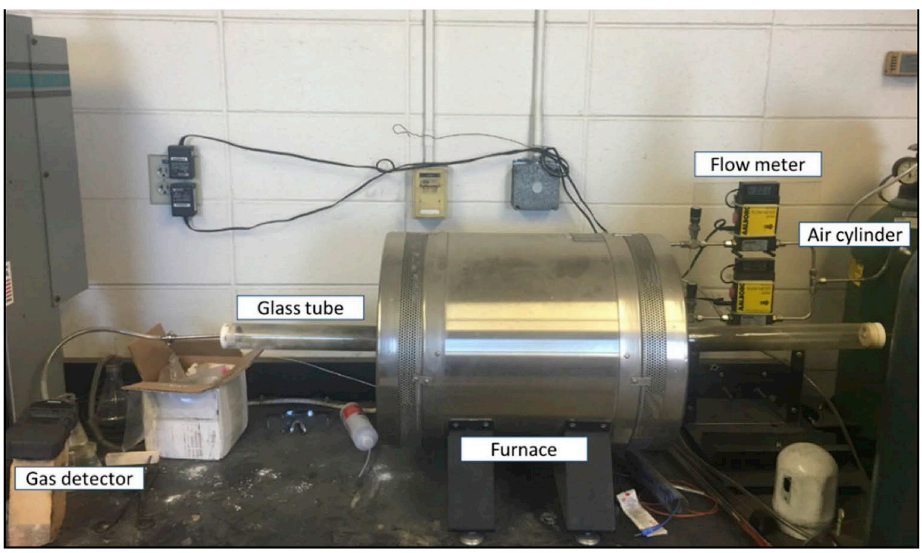

Fig. 5. Experimental setup for combustion studies.

4. Results and discussion

Data obtained from the experiments was analyzed to observe any anomalies due to experimental errors. The data exhibited the expected trend with gas concentrations increasing as the temperature in the furnace surges and the concentrations reduce to zero with the complete combustion of the specimen. Predominantly, carbon-monoxide with nominal nitrogen dioxide concentrations were detected in all the specimens. Hence, the emission factors for carbon-monoxide were calculated.

4.1. Heat of combustion

The heat release rate is the rate at which the energy is released by a specific fire of interest (NIST). It is a crucial parameter for establishing the state of a fire, the flame spreading rate and smoke production (Kang, Qin, Han, & Cong, 2019). Methods used to evaluate the heat release rate include a technique based on mass balance if heat of the combustion of fuel is available, and the calorimetric method in the absence of knowledge of the heat of combustion. Calorimetric methods are based on oxygen consumption or carbon-dioxide generation. These methods are based on the fact that the amount of energy released per unit of O_2 consumed, or CO_2 produced, is constant for a large number of materials (Biteau et al., 2008). The oxygen consumption method was used to obtain the heat of combustion for this study. Calculation of the heat release rate involves the mass flow rate, gas concentration, and temperature obtained from the experiment. The formula used for calculating the heat release rate is given below (Hansen & Ingason, 2013):

$$Q = \frac{13{,}100 \times \rho o \times uo \times A \times (M_{O2}/M_a) \times (1 - X_{H2o,o})}{\left(\frac{0.1}{X_{o2,0}}\right) + \left[\left(1 - X_{O2,avg}\right) \times \left(X_{O2,avg}\Big/\left(1 - X_{Co2,avg}\right)\right) \Big/ \left(X_{O2,O} - \left(X_{o2,avg} \times \left(\frac{1 - X_{Co2,o}}{1 - X_{Co2,avg}}\right)\right)\right)\right]}$$

where:

Q- heat release rate (kW)
ρo − ambient air density (0.567) $\left(\frac{kg}{m^3}\right)$,
uo − cold gas velocity (4.63 E− 04) $\left(\frac{m}{s}\right)$,
A − cross sectional area (1.52 E− 03) (m^2),

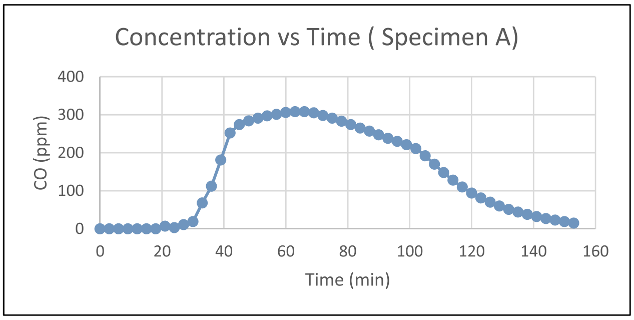

Fig. 6. Concentration vs time graph for specimen A.

M_{O2} − molecular weight of oxygen (32) (g/mol),
M_a − molecular weight of air (28.95) (g/mol),
$X_{H2o,o}$ − mole fraction of water in the ambient air,
$X_{o2,0}$ − mole fraction of oxygen in the ambient air ,
$X_{O2,avg}$ − average concentration of oxygen,
$X_{Co2,avg}$ − average concentration of carbon dioxide ,
$X_{Co2,o}$ − mole fraction of carbon dioxide in the ambient air,

Heat release rate for all four specimens depends on the average concentration of oxygen and carbon dioxide, as other parameters are constant for the specimens. Heat release rate for all the four specimens was calculated as 2.1877 kJ/kg. These materials are made of fire-resistant substance and observation of the burning cycle established the fact that not much heat was released during the process. The material smolders and does not produce flame through the burning process which is an advantage in any firefighting situation.

4.2. Emission factor

The emission factor is defined as the total mass of a pollutant emitted to the mass of fuel consumed (Maynard, Hosseini, Princevac, & Mahalingam, 2009). It is one of the input parameters required for fire modeling using commercial mine ventilation software packages. The mathematical expression for the emission factor is:

$$EF_x(\mathrm{g\ kg^{-1}}) = \frac{m_x}{m_{\mathrm{burned}}}$$

where, EF_x is the emission factor of compound X, m_{burned} is the mass of dry fuel consumed (kg), and $m_x$is the total mass of pollutant emitted (g) which is given by the expression:

$$m_x = \int_{to}^{t} \Delta\, Q_{\mathrm{duct}}\, \mathrm{d}t$$

$$m_x = Q_{\mathrm{duct}} \int_{to}^{t} \Delta C_x$$

where, ΔC_X is the concentration of the pollutant measured within the stack platform, Q_{duct} is the volumetric flow rate through the exhaust duct ($m^3 s^{-1}$), t_o is time to ignition (s), and t is the time at the conclusion of smoldering (Maynard et al., 2009). This equation is evaluated using the trapezoid rule for data. First, the concentration versus time plots were obtained for all the specimens. Figs. 6-9- show the plots obtained for specimens A, B, C, and D, respectively. Next, the concentration of carbon-monoxide is transformed into mg/$m^3$for 350 °C. Furthermore, the concentration is multiplied by the volumetric flow rate to obtain the integrand. A MATLAB function was generated to perform this integration, which used time (x value) and concentration (y value) as inputs, additionally the final integration value for expression was obtained as an output for this code. Appendix 1 shows the MATLAB code used for this calculation. Table 1 shows the mass of dry fuel consumed and the emission factors for all the specimens.

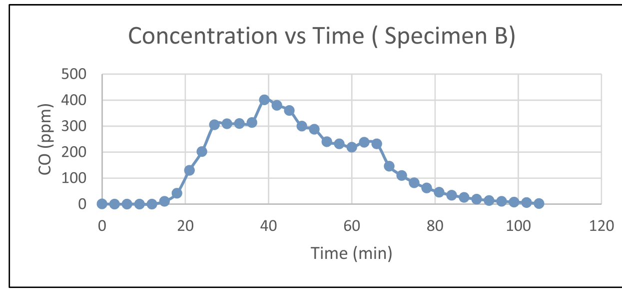

Fig. 7. Concentration vs Time graph for specimen B.

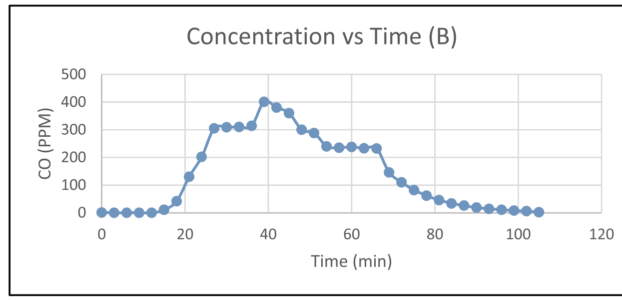

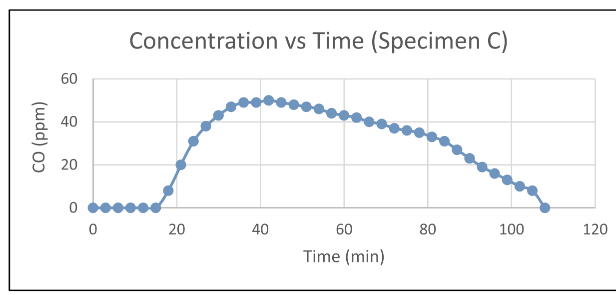

Fig. 8. Concentration vs Time graph for specimen C.

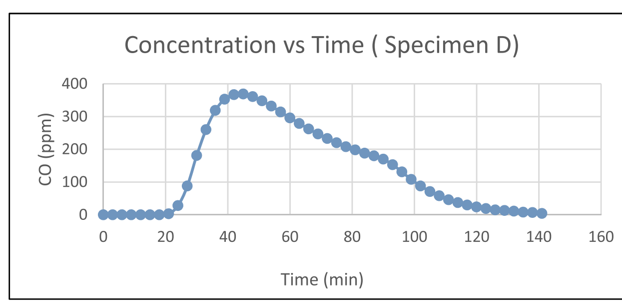

Fig. 9. Concentration vs Time graph for specimen D.

5. Conclusions

A novel approach to calculate the heat release rate and emission factors for ventilation ducts is presented in this paper. Differential scanning

Table 1
Emission factor for specimens.

Specimen	Mass of fuel consumed (g)	m_x (g)	Emission factor (g/g)
A	0.08	0.0501	0.63
B	0.12	0.0354	0.30
C	0.02	0.0069	0.35
D	0.04	0.0446	1.12

calorimetry and thermogravimetric analysis were utilized in the preliminary investigation of the ducts. In addition, a novel experimental setup was used to conduct the combustion experiment and products of combustion were monitored throughout the experiment until no detectable gases were observed. Furthermore, the heat release rate of the specimens was calculated using the oxygen consumption method and identical values were obtained, as the oxygen consumed for each of the samples was almost the same. Also, the emission factors for all the specimens were calculated and sample B was found to have the lowest emission factor for carbon-monoxide. This study provides useful information for future fire modeling studies.

Ethical statement

Authors state that the research was conducted according to ethical standards.

Funding body

National Institute For Occupational Safety and Health.

Conflicts of interest

None declared.

Acknowledgments

The authors acknowledge the financial support from the National Institute for Occupational Safety and Health (NIOSH) (No. 200-2014-59613) for conducting this research.

Appendix A

```
%%%%%%%%%%%%%%%%%%%%%%%%%%%%%%%%%%%%%%%%
% May 22, 2019
%trapezoid_data,

% Estimates the integral of a data by using the x_vals and y_vals...
% for of the data

% Inputs:
%x_vals: x values of the data
%y_vals: y values of the data

% Outputs:
% integral: the integral result for the data
%%%%%%%%%%%%%%%%%%%%%%%%%%%%%%%%%%%%%%%%%%%%%%%%%%%%%%%%%%%%%
% Initialize the different variable required in the program
function [integral]=trapezoid_data(x_vals,y_vals)

% if statement to check inputs in function
if (nargin<2)
error(['Error!, atleast two argument required,'...
'check that you have provided, x_vals,andy_vals,'])
end

% initialize the order or x_vals and y_vals
x_vals_order=size(x_vals);
y_vals_order=size(y_vals);

% if to check if x_vals and y_vals are colummn vector
if(x_vals_order(2)~=1)
error(['Error, x_val is not a column vector,'...
'enterx_val as a column vector'])
end
if(y_vals_order(2)~=1)
error(['Error, y_val is not a column vector,'...
'entery_val as a column vector'])
end
% if to check if x_vals and y_vals are of same length
if(x_vals_order(1)~=y_vals_order(1))
error(['Error, x_val and y_val are not of same length,'...
'providex_val, and y_val of the same length'])
end
% initialize sum and check the num_slices are not zero
sum=0;

% for loop to calculate the area under the data points

fori=1:(x_vals_order(1)-1)
    sum=sum+(1/2)*(y_vals(i,1)+y_vals(i+1,1))*(x_vals(1+i,1)-x_vals(i,1));
disp(sum)
end
integral=sum;
disp(integral)
end
```

References

Ajitha, S. S., Bhargava, R., Pan, Y., Jha, A., Tukkaraja, P., Shahbazi, K., ... Loring, D. (2019). A preliminary experimental investigation of the airflow resistance of an evolving cave in a block/panel cave mine. *Paper presented at the proceedings of the 11th international mine ventilation congress*.

Alagarsamy, P. (2016a). Differential scanning calorimetry, and thermogravimetric analysis. *Characterization of Material, 2018*. Retrieved May 20, 2019 from https://nptel.ac.in/courses/115103030/22.

Alagarsamy, P. (2016b). Interpretation of TGA curves. Thermogravimetric analysis. Retrieved May 20, 2019 from https://nptel.ac.in/courses/115103030/23.

Alagarsamy, P. (2016c). *Thermogravimetric analysis. Module 4 : Thermal analysis, 2019.* Retrieved May 20, 2019 from https://nptel.ac.in/courses/115103030/23.

Arya, S., Novak, T., Saito, K., Levy, A., & Sottile, J. (2019). Empirical formulae for determining pressure drop across a 20-layer flooded-bed scrubber screen. *Min. Metall. Explor.* 1–9.

Biteau, H., Steinhaus, T., Schemel, C., Simeoni, A., Marlair, G., Bal, N., et al. (2008). Calculation methods for the heat release rate of materials of unknown composition. *Fire Safety Science, 9*, 1165–1176. https://doi.org/10.3801/iafss.Fss.9-1165.

Brake, D. (2013). Fire modelling in underground mines using ventsim visual Vent FIRE software. *Paper presented at the Proceedings of the Australian mine ventilation conference, Adelaide, SA, Australia*.

Consulting, C. Ventsim Visual™ user guide In Vol. 1. Howden (Ed.).

Conti, R. S. (2001). Responders to underground mine fires. *Paper presented at the 32nd annual conference of the Institute on mining health safety and research, Salt lake city*.

Conti, R. S., Chasko, L. L., Wiehagen, W. J., & Lazzara, C. P. (2005). Fire response preparedness for underground mines. Retrieved May 24, 2019 from Cincinnati, Ohio https://www.cdc.gov/niosh/mining/UserFiles/works/pdfs/2006-105.pdf.

Dozolme, P. (2019). *Specific and non-specific hazards in underground mines.* Retrieved May 24, 2019 from https://www.thebalancesmb.com/specific-and-non-specific-hazards-in-underground-mines2367338.

Duckworth, I. (2008). Fires in vehicular tunnels. In K. Wallace (Ed.). *Proceedings 12th US/North American mine ventilation Symposium, Reno* (pp. 393–400). .

Egan, M. R. (1990). *Summary of combustion products from mine materials: Their relevance to mine fire detection. Information circular, Vol. 9272*. Washington, DC: U.S. Bureau of Mines.

Gangrade, V., Schatzel, S. J., & Harteis, S. P. A. (2019). A Field Study of Longwall Mine Ventilation Using Tracer Gas in a Trona Mine. *Mining, Metallurgy & Exploration, 36*(6), 1–11. https://doi.org/10.1007/s42461-019-0096-0.

Hansen, R., & Ingason, H. (2013). Heat release rate measurements of burning mining vehicles in an underground mine. *Fire Safety Journal, 61*, 12–25. https://doi.org/10.1016/j.firesaf.2013.08.009.

Jha, A., Calizaya, F., & Nelson, M. G. (2015). Spontaneous combustion prediction and remediation techniques. *Paper presented at the 15th North American mine ventilation Symposium, Blacksburg*.

Jha, A., & Tukkaraja, P. (2019). Monitoring and assessment of underground climatic conditions using sensors and GIS tools. *Paper presented at the 17th North American mine ventilation Symposium, Montreal*.

Kang, N., Qin, Y., Han, X., & Cong, B. (2019). Experimental study on heat release rate measurement in tunnel fires. *Fire and Materials, 43*(4), 381–392. https://doi.org/10.1002/fam.2710.

Kumar, A. R., Wedding, W. C., Jolly, A., Arya, S., & Novak, T. (2016). Modeling capture efficiency for a flooded bed dust scrubber incorporated into a longwall shearer using a small scale physical model and CFD. *Paper presented at the SME annual conference & Expo, phoenix, AZ*.

Laboratory, M. T. (2012). *Differential Scanning Calorimetry (DSC) – online training course*.

Lazzara, C., & Perzak, F. (1990). Conveyor belt flammability studies. *Proceedings: 21st Annual Institute on Coal Mining Health, Safety, and Research,* 28–30.

Maynard, T., Hosseini, E., Princevac, M., & Mahalingam, S. (2009). *Laboratory-based experimental measurement of particulate emission factor for wildland fuels*.

McPherson, M. J. (2012). *Subsurface ventilation and environmental engineering, Vol. I*. New Delhi, India: Springer Science & Business Media.

Mining Product: MFIRE. Retrieved June 4, 2019 from https://www.cdc.gov/niosh/mining/works/coversheet1816.html.

MSHA (2019). *U.S. mining fatalities in 2018 were second lowest on record.* Retrieved June 4, 2019 from https://www.msha.gov/news-media/press-releases/2019/01/09/us-mining-fatalities-2018-were-second-lowest-record.

NIST Fire dynamics. Retrieved June 4, 2019 from https://www.nist.gov/el/fire-research-division-73300/firegov-fire-service/fire-dynamics.

NIST Fire dynamics simulator (FDS) and smokeview (SMV). Retrieved June 8, 2019 from https://pages.nist.gov/fds-smv/.

PerkinEmler, I. Thermogravimetric analysis (TGA). Retrieved June 8, 2019 from https://www.perkinelmer.com/lab-solutions/resources/docs/FAQ_Beginners-Guide-to-Thermogravimetric-Analysis_009380C_01.pdf.

Prosser, B., Briones, S. V., Van Diest, J., Zuñiga, R. A., Marin, A. G., & Barrena, G. L. (2017). Development of A fire modeling study for the chuquicamata underground mine. *Paper presented at the 16th North American mine ventilation Symposium, Golden,CO*.

Rosa, M. I. D. (2004). *Analysis of mine fires for all U.S. Underground and surface coal mining categories: 1990-1999.* Retrieved June 8, 2019 from https://www.cdc.gov/niosh/mining/UserFiles/works/pdfs/2004-167.pdf.

Thermal Analysis Instruments (2010). *Thermal analysis.* Retrieved May 26, 2019 from http://www.tainstruments.com/wp-content/uploads/BROCH-THERMAL-2015-EN.pdf.

Trevits, M. A., Yuan, L., Smith, A. C., & Thimons, E. D. (2008). NIOSH mine fire research in the United States. *Paper presented at the Ninth International Mine Ventilation Congress, New Delhi*.

Wikipedia Differential scanning calorimetry 2019. Retrieved June 17, 2019 from https://en.wikipedia.org/wiki/Differential_scanning_calorimetry.